



Contents lists available at SciVerse ScienceDirect

# Journal of Wind Engineering and Industrial Aerodynamics

journal homepage: [www.elsevier.com/locate/jweia](http://www.elsevier.com/locate/jweia)

## Aerodynamic characteristics of a tube train

Tae-Kyung Kim<sup>a</sup>, Kyu-Hong Kim<sup>b,\*</sup>, Hyeok-Bin Kwon<sup>c</sup><sup>a</sup> Department of Mechanical and Aerospace Engineering, Seoul National University, Seoul 151-744, South Korea<sup>b</sup> Institute of Advanced Aerospace Technology, Seoul National University, Seoul 151-744, South Korea<sup>c</sup> High-Speed Railroad Systems Research Center, Korea Railroad Research Institute, #176, Cheoldo bangmulgwan-ro, Uiwang, Gyeonggi-do 437-757, South Korea

### ARTICLE INFO

#### Article history:

Received 15 March 2010

Received in revised form

2 February 2011

Accepted 1 September 2011

Available online 20 October 2011

#### Keywords:

Tube train

Tube transport system

Tube transportation

Tube vehicle

Vacuum tube transportation

### ABSTRACT

Recently, full-scale research about a passenger tube train system is being progressed as a next-generation transportation system in Korea in light of global green technology. The Korea Railroad Research Institute (KRRRI) has commenced official research on the construction of a tube train system. In this paper, we studied various parameters of the tube train system such as the internal tube pressure, blockage ratio, and operating speed through computational analysis with a symmetric and elongated vehicle. This study was about the aerodynamic characteristics of a tube train that operated under standard atmospheric pressure (open field system, viz., ground) and in various internal tube environments (varying internal tube pressure, blockage ratio, and operating speed) with the same shape and operating speed. Under these conditions, the internal tube pressure was calculated when the energy efficiency had the same value as that of the open field train depending on various combinations of the operating speed and blockage ratio (the  $P$ - $D$  relation). In addition, the dependence of the relation between the internal tube pressure and the blockage ratio (the  $P$ - $\beta$  relation) was shown. Besides, the dependence of the relation between the total drag and the operating speed depending on various combinations of the blockage ratio and internal tube pressure (the  $D$ - $V$  relation) was shown. Also, we compared the total (aerodynamic) drag of a train in the open field with the total drag of a train inside a tube. Then, we calculated the limit speed of the tube train, i.e., the maximum speed, for various internal tube pressures (the  $V$ - $P$  relation) and the critical speed that leads to shock waves under various blockage ratios, which is related to the efficiency of the tube train (the critical  $V$ - $\beta$  relation). Those results provide guidelines for the initial design and construction of a tube train system.

© 2011 Elsevier Ltd. All rights reserved.

### 1. Introduction

A tube train system is a high-speed ground vehicle through a sealed tube or tunnel. Regarding travel in a sealed and sub-vacuum tube, aerodynamic noise that propagates to the ambient environment is shielded and energy efficiency is increased through a decrease in the total or aerodynamic drag (Kim, 2008; Retrieved 23.05.07.; Retrieved 23.04.07.). The tube system originated from a Pneumatic Capsule Pipeline (PCP) system. After the PCP system was officially proposed by the English businessman, George Medhurst, in 1810, a variety of studies and actual construction were undertaken. After the first proposition, the constructed PCP system for which the driving force was the pressure difference in the tube has been used for small-cargo haulage in the US, the UK, and France. PCP transport for personnel also has been studied, but not been built as yet (Retrieved

03.05.09.; Retrieved 03.05.09.). This system rose to prominence in the late 1960s and early 1970s during the first oil shock. In recent times, the PCP system has attracted renewed interest in the light of energy and environmental concerns. Hence, studies of small vehicles for personnel and cargoes in the tube train or capsule system have been performed in the US, Germany, Italy, Switzerland, and so on (Retrieved 29.05.07.; Retrieved 06.12.07.; Retrieved 05.12.07.; Retrieved 24.04.07.). In those studies, Swissmetro proposed and studied a tube train system based on a magnetic levitation (maglev) train for the large-scale transportation of personnel (Retrieved 23.05.07.). The Korea Railroad Research Institute (KRRRI) also has commenced official research on a tube train system based on a maglev train traveling at 700–1000 km/h for the construction of a passenger tube train system. However, systematic research about the aerodynamic characteristics of such a high-speed tube train system is rather scant (Kwon et al., 2008; Lee et al., 2008; Kwon, 2008).

The most intensive study about the aerodynamic analysis and energy efficiency of a tube system was conducted from September 1966 through October 1969 in a project undertaken by the US Transportation Bureau; the experimental results were published

\* Corresponding author. Tel.: +82 2 880 8920; fax: +82 2 880 8302.

E-mail addresses: [dukektk@hanmail.net](mailto:dukektk@hanmail.net) (T.-K. Kim), [aerocfd1@snu.ac.kr](mailto:aerocfd1@snu.ac.kr) (K.-H. Kim), [hbkwon@krri.re.kr](mailto:hbkwon@krri.re.kr) (H.-B. Kwon).

## Nomenclature

$\beta$	blockage ratio
$A$	area of the train
$C_p$	pressure coefficient
$C_D$	drag coefficient
$C_{D,p}$	pressure drag coefficient
$C_{D,v}$	viscous drag coefficient
$V$	velocity
$T$	temperature

$P$	pressure
$D$	diameter of tunnel
$\rho$	density
$\mu$	viscosity of air
$\gamma$	specific heat ratio
$R$	specific gas constant
$a$	speed of sound
$V_C$	critical speed
$M$	Mach number
Re	Reynolds number

in 1970 (Trzaskoma, 1970). According to this study, the drag coefficient ( $C_D$ ) of a vehicle is about 0.015–0.11 when the vehicle has a semicircular nose and rear under the atmospheric internal tube pressure condition. The Reynolds number (Re) is  $10^5$  and the blockage ratio is one of 0.125, 0.22, 0.38, and 0.5. Harman and Davidson (1977) compared  $C_D$  under the wind-tunnel condition with  $C_D$  under the moving-vehicle condition. An ogive-shaped vehicle was used and Re was  $10^5$ . The blockage ratio was varied from 0.6 to 0.9 under the internal tube condition of about one atm (14.5 psia) and  $74^\circ$  (296.5 K) (Harman and Davidson, 1977). However, those experiments had limitations and showed only a trend in  $C_D$  because the tube train model had a simple geometry; a semicircular nose and an ogive rear, and had a relatively short length (the ratio of the length to diameter was 8.85). Furthermore, those experimental conditions and data were not suitable for the recently required tube train systems that operate at a Mach number of 0.6 and internal tube pressure of 0.01 atm, because the maximum operating speed of the experimental vehicle model was a Mach number of 0.4 or less and the internal tube pressure was the atmospheric condition of about one atm. In a doctoral dissertation at Ecole polytechnique fédérale de Lausanne (EPFL) in 1999, a relationship between the pressure waves and aerodynamic drag in a tunnel was studied through the Swissmetro model (Bourquin and Alexis Monkewitz, 1999). However, this study needs to be complemented for accuracy because the numerical models used were a 1-D unsteady pressure-wave model and a 1-D laminar unsteady friction model with heat transfer. It said that these models had not enough accuracy itself for prediction of drag with an unsteady flow pattern in a long tunnel and it is necessary to combine 3-D numerical computation to obtain the overall drag and its components on a high-performance train.

Thus, in this paper, we studied the aerodynamic drag of a tube train by changing important initial design variables such as the blockage ratio, internal tube pressure, and operating speed. A full-scale investigation of the tube train system was conducted for the initial design state. Since experimental analysis has limitations with regard to geometry, temperature, pressure, and operating speed, we performed computational analysis based on unsteady compressible Navier–Stokes equations. These study results, which include various driving aerodynamic drag data and the trend of  $C_D$  with respect to each blockage ratio, internal tube pressure, and

operating speed, will provide guidelines for the construction of a tube train system and related research.

## 2. Method

Generally, the assumption of incompressible flow is applied for the calculation of the aerodynamic drag of a ground vehicle because most vehicles operate at speeds of less than 300 km/h. However, the current high-speed transportation systems, such as High Speed Rail (HSR), Maglev trains, and aircraft, operate at 300 km/h or higher. Thus, these transportation systems should consider the compressibility effects of air. In addition, a tube train is to be operated with very high speed inside the tube, which has a restricted environment. Hence, in the case of a tube train, the consideration of the compressibility effects leads to a very large variation in the results.

### 2.1. Governing equations

The governing equations are 2nd-order unsteady compressible Navier–Stokes equations in an axisymmetric two-dimensional coordinate system (Kwak, 1990).

The Sutherland two-equation viscous model and the  $k-\omega$  Shear Stress Transport (SST) turbulence model proposed by Menter were used (Kwak, 1990). Table 1 shows the physical values of internal tube and vehicle when four different turbulence models were used. The time averaged total drag force, which is the one of the main factors in the present paper, is compared with each other. Each case is the same conditions as blockage ratio 0.25, internal pressure 0.01 atm, internal temperature 288.15 K and operating speed 2000 km/h.

The values of turbulence model are a little bit different from each other. Thus,  $k-\omega$  SST was selected in this paper (Table 2).

The Implicit Roe's Flux Difference Scheme (FDS) was used for spatial discretization and Monotone Upstream-centered Schemes for Conservation Laws (MUSCL), which explicates the physical variables, was used to extend the spatial accuracy to the third order.

For time integration, the dual time stepping scheme was adopted to enhance the time accuracy for the analysis of the unsteady flow field.

**Table 1**  
Comparison of turbulence models.

Turbulence model	Average max. Mach number	Average max. static temp. (K)	Average max. static press. (atm)	Average pressure drag force (kN)	Average viscous drag force (kN)	Average total drag force (kN)	Error (%)
$k-\omega$ SST	2.120	752.583	0.036575	106.554	7.837	114.391	–
$k-\varepsilon$	2.202	661.922	0.036384	106.948	8.644	115.592	1.05
Spalart–Allmaras	2.157	703.885	0.037456	104.529	7.928	112.457	1.69
Laminar	2.216	736.732	0.038867	107.135	2.884	110.019	3.82

**Table 2**  
Results of grid convergence test.

Mesh (X × Y)	Average max. Mach number	Average max. static temp. (K)	Average max. static press. (atm)	Average pressure drag force (kN)	Average viscous drag force (kN)	Average total drag force (kN)	Error (%)
770 × 100	2.120	752.583	0.036575	106.554	7.837	114.391	–
1540 × 200	2.145	673.250	0.036973	105.531	8.036	113.567	0.72
385 × 50	2.143	805.209	0.035123	109.031	7.568	116.599	1.93



**Fig. 1.** Schematic of computation domain of tube train system.

Parallel computing with eight CPUs was performed by the Message Passing Interface (MPI) technique, and the implicit solution was applied for repeated calculations (Kwak, 1990; Sung Kim, 2001; Lee and Lee, 1998; Rumsey et al., 1995; Arnone et al., 1995).

## 2.2. Boundary conditions and assumptions

The gases of the open field and inside the tube were assumed as an ideal gas. For initial conditions, the internal temperature of tube was initially given 288.15 K in all cases. However, the pressure and flow speed were set differently depending on the specific case. In this paper, friction or drag refers to only aerodynamic drag and excludes rolling friction under wheel and rail.

The boundary condition of the open field system and the entrance of the tube train system were set to 'pressure far field'. Hence, the inflow pressure, velocity, and temperature were fixed. For a tube system, the non-reflecting boundary condition was applied to the tube exit to minimize a non-physical reflected pressure wave. Especially, in order to remove the effect of reflected pressure wave clearly, the length of tube was sufficiently long so that the pressure wave which propagated from a train did not reach the tube exit during computations.

The vehicle surface was a stationary wall and the no-slip condition was applied. The inside wall of the tube was set to a moving wall that had the same speed as the inflow. Through those wall conditions, the vehicle movement was described without real wall movement and the unnecessary flow effect due to the interaction between the vehicle wall and the inner tube wall was minimized. The bottom line of the grids was the axis and the top line of grids was rotated around the  $x$ -axis.

## 2.3. Mesh

The grid geometry of the tube train was based on a model of the Transrapid International Maglev Train, which was manufactured by the German company, Siemens, and ThyssenKrupp. This train has been the current worldwide commercially used maglev train with a speed of 500 km/h and has operated in Shanghai (Retrieved 20.08.08.). Detailed specifications of the train geometry are as follows: a height of 3.7 m, length of 51.7 m, and  $l/d$  about 14, for two carriages.

The open system describes the field under ambient pressure with 50,000 grid points and is named, the 'Open Field System', in Fig. 1. The distance from the wall of the vehicle to the far boundary is 517 m, which is ten times the vehicle length. The tube train system describes the tube or tunnel with the train

inside the tube using 77,000 grid points. The train length is 51.7 m. Three types of shape are classified by the blockage ratio, when the upper tube wall is rotated around the  $x$ -axis. The blockage ratio is represented by Eq. (1)

$$\text{Blockage ratio } (\beta) = \frac{\text{cross sectional area of vehicle}}{\text{cross sectional area of tunnel}} \quad (1)$$

The grid points were resized to one fourth and four times points for a grid convergence test and time averaged total drag forces were compared each other. Each initial condition is the same as blockage ratio 0.25, internal pressure 0.01 atm and operating speed 2000 km/h.

The result of (1540 × 200) mesh was similar with that of (770 × 100) mesh. However, the average total drag of (385 × 50) mesh had about two percentage differences. Thus, (770 × 100) mesh was selected in this paper.

## 3. Results

The three most important initial design parameters of the tube train system are the blockage ratio, internal tube pressure, and tube train operating speed. The aerodynamic drag of the tube train system needs to be compared directly or indirectly with the aerodynamic drag of current and similar transportation systems for finding the minimum operating-condition requirements of a tube train system that has the three variables stated above. Hence, in the present study, two variables needed to be fixed; then, the remaining variable was varied to examine its effect on the aerodynamic drag or the total drag. For example, the results of Section 3.1 show the total drag with respect to the internal tube pressure under a constant blockage ratio and operating speed. Also, the results of Section 3.2 show the total drag for various operating speeds under a constant blockage ratio and internal tube pressure. In addition, the total drag of the open field system was compared with the total drag of the tube train in Fig. 1. The primary results were as follows.

- (1) The  $P$ - $D$  relation, viz., the relation between the internal tube pressure and the velocity-blockage ratio when the time averaged aerodynamic drag of the operating tube train had the same value as that of the open system.
- (2) The  $P$ - $\beta$  relation, viz., the relation between the internal tube pressure and the blockage ratio.
- (3) The  $D$ - $V$  relation, namely, the relation between the time averaged aerodynamic drag of the tube train and the

operating speed for various cases of the blockage ratio-internal tube pressure.

- (4) The  $V$ - $P$  relation, i.e., the relation between the speeds (the limit speed and the operating speed) of the tube train and the internal tube pressure, which is required for the design of a tube train system.
- (5) The critical  $V$ - $\beta$  relation, which is the relation between the critical speed of the tube train and the blockage ratio when the Mach number of the local flow around the vehicle reaches unity.

3.1. Internal tube pressure depending on the velocity-blockage ratio

Tables 3 and 4 show the average drag of the open field train (ground maglev) under the standard pressure condition for speed levels of 500 and 700 km/h. They also show the internal tube

pressure when the average drag of the tube train system has the same value as that of the open field train ('Open sys.' in tables) according to the blockage ratio with speed levels of 500 and 700 km/h, respectively. Aerodynamic drag of the open system was validated by that of two different maglev which were Bechtel and Transrapid (TR07) (Lever, 1998). Fig. 2 shows that the cross-sectional areas of Bechtel are similar to a circle but that of TR07 are similar to a square. The result of the open system in the present paper has the similar value to that of Bechtel because both are axisymmetric shapes and have similar cross-sectional areas. The difference between two results was about 6.887%, which could be accepted in consideration of the difference of train nose shape.

Lines 1 and 2 in Fig. 3 show that the total drag is linearly proportional to the internal tube pressure when the tube train has a blockage ratio of 0.25 and operating speeds of 500 and

**Table 3**  
The internal tube pressure when the time averaged total drag of the tube train is the same as the total open-system drag depending on the velocity (500 km/h) and blockage ratio.

Blockage ratio	Train operating speed (km/h)	Pressure (atm)	Average maximum Mach number	Average pressure drag force (N)	Average viscous drag force (N)	Average total drag force (N)	Difference in the total drag force (%)
Open sys.	500	1.0	0.554	13,559.6	30,482.7	44,042.3	–
TR07		1.0	–	–	–	57,600.0	23.53
Bechtel		1.0	–	–	–	47,300.0	6.887
0.25		0.05315	0.628	40,145.9	3763.8	43,909.7	0.302
0.5		0.021	0.944	42,124.4	2572.0	44,696.4	1.463
0.75	0.011546	1.409	41,595.5	1947.3	43,542.9	1.147	

**Table 4**  
The internal tube pressure when the time averaged total drag of the tube train is the same as the total open-system drag depending on the velocity (700 km/h) and blockage ratio.

Blockage ratio	Train operating speed (km/h)	Pressure (atm)	Average maximum Mach number	Average pressure drag force (N)	Average viscous drag force (N)	Average total drag force (N)	Difference in the total drag force (%)
Open sys.	700	1.0	0.834	29,669.1	54,102.7	83,772.8	–
0.25		0.05	1.194	79,144.9	6185.8	85,330.7	1.826
0.5		0.022	1.631	79,184.3	3896.3	83,080.7	0.833
0.75		0.015	1.912	82,789.1	3426.5	86,215.6	2.833

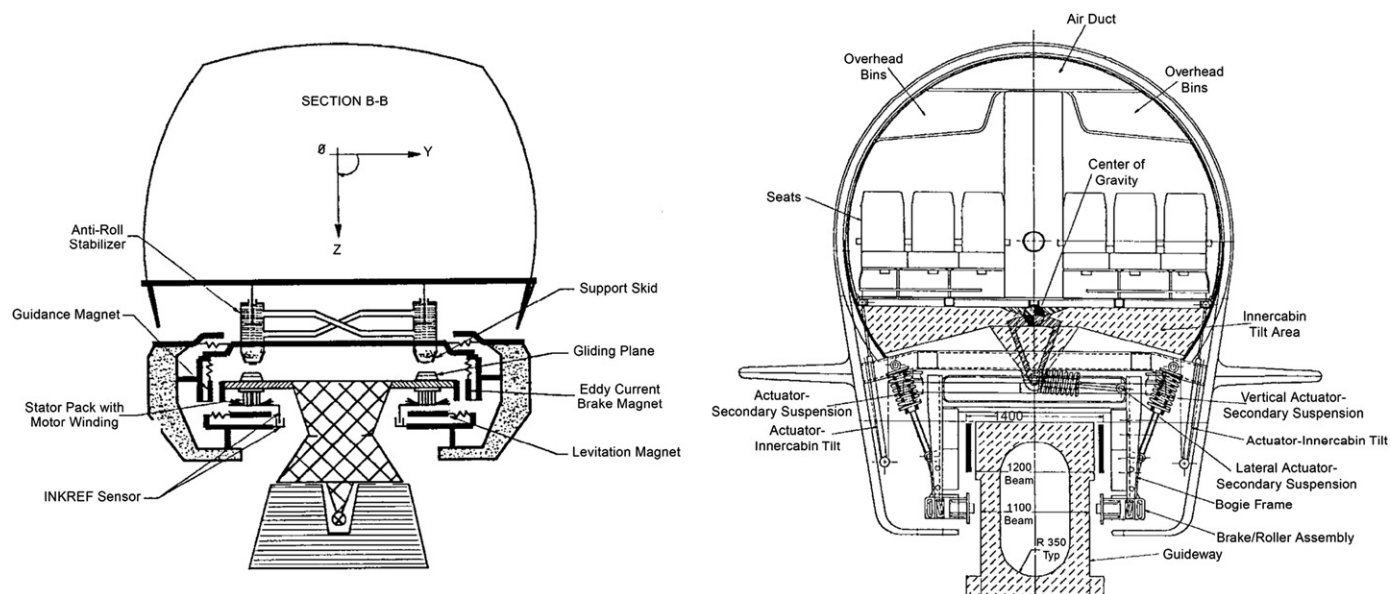


Fig. 2. Transrapid (TR07) and Bechtel.



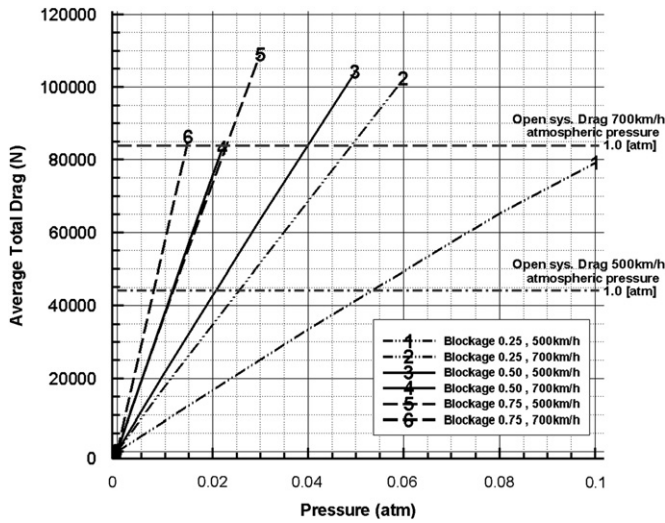


Fig. 3. The internal tube pressure vs. the time averaged total drag for a blockage ratio of 0.25 to 0.75 and velocities of 500 and 700 km/h.

700 km/h, respectively. The horizontal dotted lines show the average total drag of the open field maglev train from ‘Open sys.’ in Tables 3 and 4. Hence, the points of intersection of the horizontal dotted lines and the two lines (lines 1 and 2) are the conditions whereby the total drag of the tube train has the same value as that of the open-field train. Those pressure values at the points of intersection are shown in Tables 3 and 4. In the same manner, lines 3, 4 and lines 5, 6 show that the total drag linearly increased as the internal tube pressure increased, when the tube train had blockage ratios of 0.5 and 0.75 and operating speeds of 500 and 700 km/h, respectively.

If the propulsion system of a ground maglev train is adopted for a tube train with a speed level of 500–700 km/h, the maximum total drag of the tube train also will be the same as that of the train in the open air. Accordingly, the internal tube pressure that generates the same drag can be found if the blockage ratio and operating speed of the tube train are given. Therefore, when the propulsion system at an operating speed of 500 km/h is chosen and the tube train operates at 500 km/h corresponding to the propulsion system, the maximum internal tube pressure is about: 0.055 atm at  $\beta=0.25$  (line 1); 0.0207 atm at  $\beta=0.5$  (line 3); and 0.012 atm at  $\beta=0.75$  (line 5). The corresponding values for an operating speed of 700 km/h are about: 0.05 atm at  $\beta=0.25$  (line 2); 0.025 atm at  $\beta=0.5$  (line 4); and 0.0145 atm at  $\beta=0.75$  (line 6) as shown in Fig. 3.

Fig. 4 shows curve fitting for the internal tube pressure based on the results of Fig. 3, which are the points of intersection. The solid line in Fig. 4 is based on three intersection points where the lower horizontal line (dash-dot line) with line 1, line 3, and line 5, respectively, in Fig. 3. It shows a specific condition of internal tube pressure when the total drag of the tube train has the same value as that of the ground maglev train with operating speeds of 500 km/h. The dot line in Fig. 4 is based on three intersection points where the upper horizontal line (dash line) with line 2, line 4, and line 6, respectively, in Fig. 3. It shows a specific condition of internal tube pressure when the total drag of the tube train has the same value as that of the ground maglev train with operating speeds of 700 km/h. Through these results, it is clearly seen that decompression of the internal tube is required to increase the blockage ratio. At both speeds, viz., 500 and 700 km/h, similar internal tube pressures are introduced to be close to 0.05 atm at  $\beta=0.25$ , 0.02 atm at  $\beta=0.5$ , and 0.01 atm at  $\beta=0.75$ , when the total drag of the tube train is the same as the total drag of a ground maglev train with the same propulsion system. Therefore,

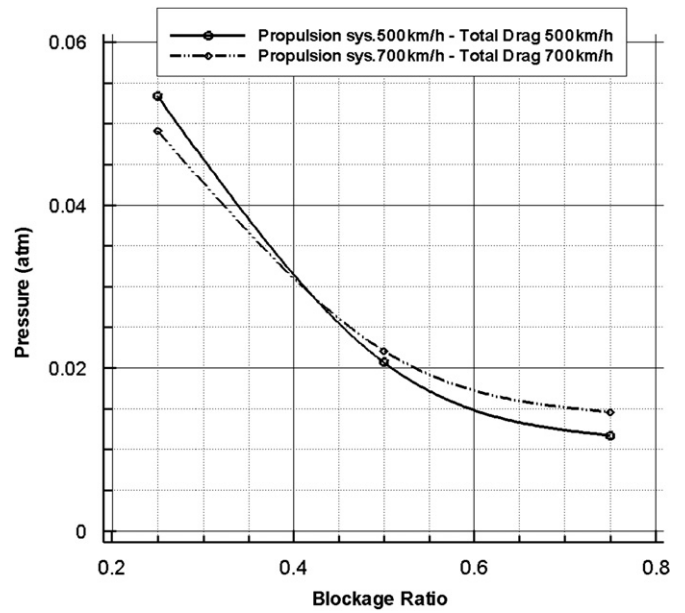


Fig. 4. The blockage ratio vs. the internal tube pressure based on the six points of intersection in Fig. 3.

it is concluded that the operating speed does not have a significant effect on the relationship between the blockage ratio and the internal tube pressure.

Generally, the driving resistance increases in proportion to the square of the operating speed. The driving resistance is composed of the pressure drag and viscous drag that are based on the vehicle shape and length, respectively. The drag on a short vehicle mostly depends on the pressure drag, but the drag on an elongated vehicle such as a train is dominated by a large viscous drag. Nevertheless, in the case of a tube train, the viscous drag is small and the pressure drag is relatively large because the internal tube pressure is at a low level. Notably, Tables 3 and 4 show that the total drag of an elongated train on the ground is composed of the pressure drag and viscous drag, and those drags are in the ratio of about 1:2. However, in a tube–train system, the ratio is approximately 10:1 (resp., 20:1) if  $\beta$  is 0.25 (resp., 0.75). Most of the total drag is pressure drag because the cross-sectional area of a tube train increases in proportion to the blockage ratio; further, the internal tube flow becomes harder to bypass because the remaining area decreases. This indicates that the effect of internal fluid increases the pressure drag and accordingly the total drag.

The pressure drag is usually proportional to the flow-density, the cross-sectional area of the vehicle, and the square of the operating speed. Among the three components, only the density plays an important role in the total drag in the case of a tube train where the cross-sectional area of the train and operating speed are fixed. As a result, the total drag was also a function of only the internal tube pressure

$$D = \frac{1}{2} \rho_{\infty} V_{\infty}^2 A C_D = \frac{1}{2} \rho_{\infty} V_{\infty}^2 A (C_{D,p} + C_{D,v}) \quad (2)$$

For a given train speed, Eq. (2) becomes

$$D = f(\rho_{\infty}, C_D) \quad (3)$$

Generally,  $C_D$  is influenced by density. However, the magnitude of it is  $O(1)$  while density varies from  $10^1$  order to  $10^{-3}$  order in a tube system. Thus,  $C_D$  can be assumed to be constant and Eq. (3) is simplified to

$$D = f(\rho_{\infty}) \quad (4)$$

Finally

$$D \propto p_{\infty} \quad (5)$$

The total drag of a tube train with constant operating speed is linearly proportional to the internal tube pressure, as shown in Fig. 3. Therefore, the internal tube pressure should be lowered for achieving the same total drag as that of a ground train even if the blockage ratio of the tube train is high.

In addition, the probability of the generation of shock waves greatly increases when the speed of accelerated flow exceeds the speed of sound. Generally, shock waves occur when the local speed of flow around a vehicle exceeds the speed of sound and they are nearby attached to a vehicle unlike Entry Compression Wave or Micro-Pressure Wave, which propagates from a vehicle. Thus, they directly affect a total drag and the efficiency reduces due to a sharp increase in the total drag or drag coefficient. Fig. 5 shows that shock waves exist at the rear train and the normal shock waves coexist with the oblique shock waves that are generated by the interaction and continuous reflection between the tube and vehicle walls. Thus, it is needed to know that how much the total drag is increased along with the strength of the shock waves. This result is summarized in Table 5. Table 5 shows the ratio of gradients (average total drag/pressure) for the six plots in Fig. 3 that feature the same operating speed but different blockage ratios; it also represents the shock strength in each case by ‘Strong’, ‘Weak’, and ‘None’. For example, the value of 2.218 represents the ratio of gradients of the two curves corresponding to the cases where  $\beta$  is 0.5 (line 4 in Fig. 3) and 0.25 (line 2 in Fig. 3), respectively, at the same speed of 700 km/h. The line 1 in Fig. 3, shock waves were not observed as shown in Table 3, under an average maximum Mach number of 0.628, while weak shock waves occurred locally in the case of line 2 with an average

maximum Mach number of 1.194, as shown in Table 4. Weak shock waves existed locally in the case of line 3 and strong shock waves existed at the rear train in the case of line 4 as shown in Fig. 5. The line 5 and line 6, both the cases exhibit strong shock waves at the rear train. Since the gradient refers to the ratio of the average total drag to the pressure, the ratio of the gradient as well as the total drag becomes the biggest in the case of a strong shock in comparison with the case of no shock waves, as shown in Table 5. This indicates that the total drag greatly increased and the efficiency sharply reduced at the appearance of shock waves.

However, if the internal tube pressure is very low, the total drag will be small, the shock effect will decrease in proportion to the pressure, and the operating speed will be faster. Consequently, if the maximum total drag of the current ground (maglev) propulsion system is the same as the drag values of ‘Open sys.’ in Tables 3 and 4, the limits on the maintainable internal tube pressure will be located at the points of intersection of the horizontal dotted lines and the six lines when the blockage ratio, propulsion system, and operating speed of the tube train system are chosen. From the viewpoint of the total drag, the operation of a tube train is impossible if the internal tube

**Table 5**

Ratio of the two gradients with the same operating speed but various blockage ratios.

Blockage ratio	Operating speed	
	500 (km/h)	700 (km/h)
0.5/0.25	2.634 (W/N)	2.218 (S/W)
0.75/0.25	4.589 (S/N)	3.375 (S/W)

S: strong shock, W: weak shock, and N: no shock.

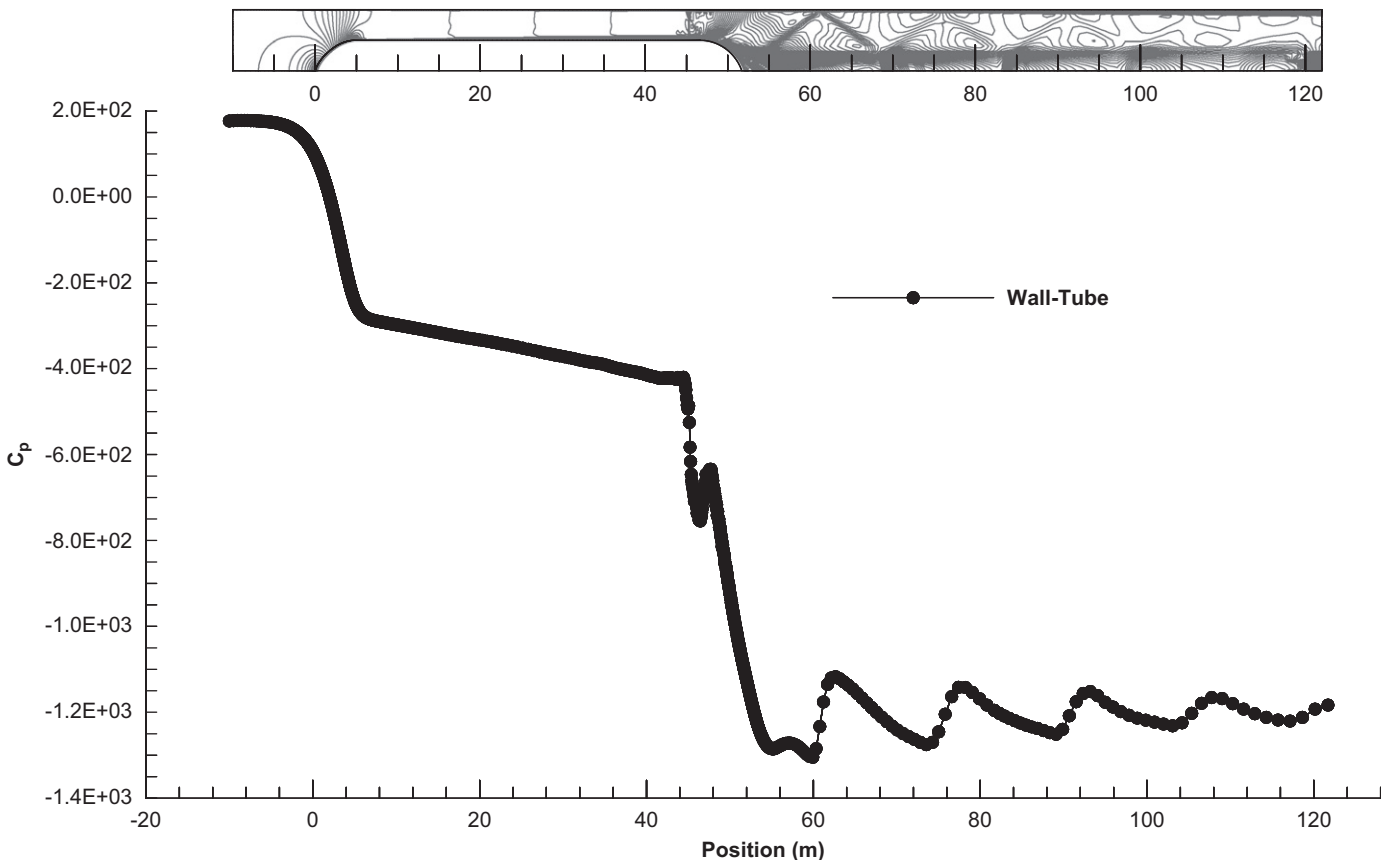


**Fig. 5.** Mach number contour and  $C_p$  along the tube wall at 7.04 s.

pressure exceeds the values at the points of intersection. In contrast, the operational efficiency of a tube train system will be at least the same or greater than that of a ground maglev train system if the pressure is below the values at the points of intersection.

3.2. The total drag and the limit speed depending on the blockage ratio and internal tube pressure

As shown in Fig. 6, the average total drag of a tube train increases in proportion to the operating speed of the tube train. These total drags are compared with those of the open field train when the blockage ratio is 0.25 and the internal tube pressure is, respectively, 0.01, 0.04, and 0.1 atm. The two horizontal lines show the average total drag of an open-field train under operating speeds of 500 and 700 km/h. When the train operates inside the tube, the average total drag rises and the drag plot intersects with the horizontal lines as the train speed increases. Also, the specific data of the points of intersection of the two lines are depicted in Fig. 7. If these operating speeds of the open-field train are the

maximum values determined from the aerodynamic drags considering the power of the propulsion system of the open-field system, the results of Fig. 7 can be defined as the limit speeds of the tube train when the equivalent propulsion power of the open-field train is adopted. If the propulsion system of the current commercial maglev train, which operates at 500 km/h, is applied to the tube train, the limit speeds of the tube train would be about 1050, 570, and 380 km/h under internal tube pressures of 0.01, 0.04, and 0.1 atm, respectively. In the same way, if we have a more powerful propulsion system that can be operated at 700 km/h in an open field, the limit speeds of the tube train can be improved to about 1600, 770, and 510 km/h, respectively, under internal tube pressures of 0.01, 0.04, and 0.1 atm, respectively. These results imply that a tube train with a speed level of about 1000 km/h can be realized with the propulsion system of current commercial maglev trains if a very low internal tube pressure or sub-vacuum can be maintained. As shown in Fig. 7, the operating speed of a tube train is much lower than the operating speed of an open-field train even when the internal tube pressure is one-tenths of the atmospheric pressure. This result is caused by the rapid augmentation of the total drag according to the effect of compressible flow and the increase in and the flow velocity, as shown in Eq. (6). In Fig. 8, the total drag of a tube train is compared with that of an open-field train depending on the operating speed when the blockage ratios are 0.5 and 0.75. An increase in the blockage ratio leads to a rise in the pressure drag, and as a result, the total drag is enormously increased even if the internal tube pressure and the operating speed are fixed. When the internal tube pressure is doubled from 0.01 to 0.02 atm without change in the blockage ratio, the total drag also increases linearly and roughly doubles. Fig. 9 shows the limit speed of a tube train with a blockage ratio of 0.5 that is obtained from the points of intersection in Fig. 8. If this tube train has the current propulsion technology of an open-field train with an operating speed of 500 km/h, the operating speed will be about 770 km/h (resp., 500 km/h) when the internal tube pressure is 0.01 atm (resp., 0.02 atm). If the propulsion power system is improved to an operating speed of 700 km/h in open ground, the operating speed of the tube train is expected to be approximately 1170 and 740 km/h, respectively, when the internal tube pressure is 0.01 and 0.02 atm.

Generally, the internal tube pressure and the blockage ratio are the most important design parameters in a tube train system

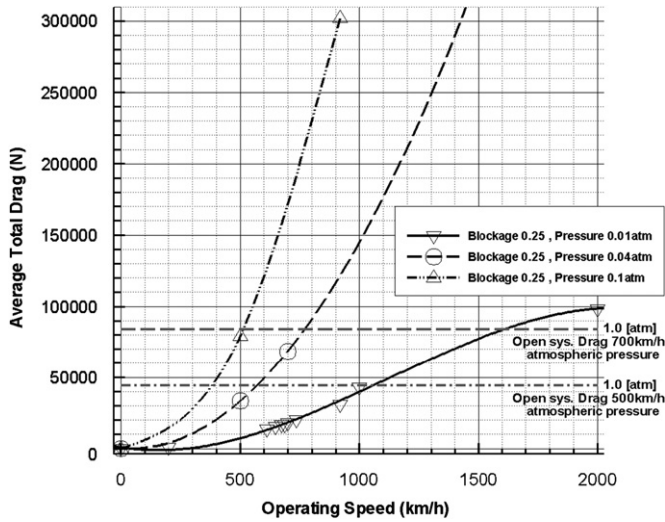


Fig. 6. Operating speed vs. the time averaged total drag with a blockage ratio of 0.25 and internal tube pressures of 0.01, 0.04, and 0.1 atm.

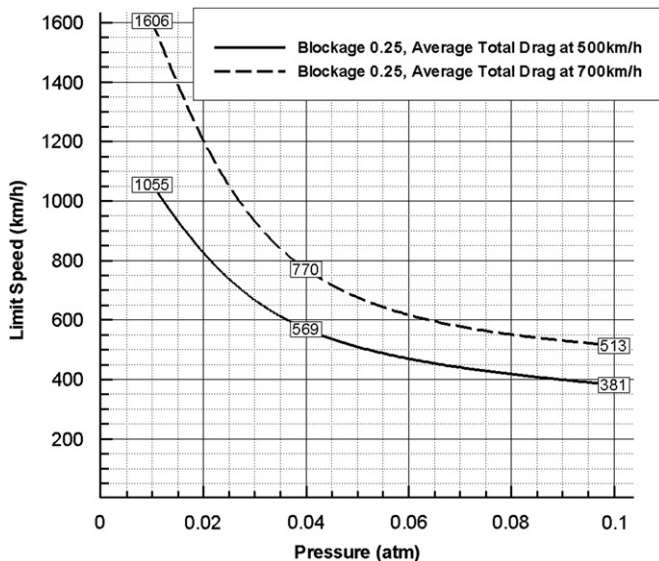


Fig. 7. The internal tube pressure vs. the limit speed with a blockage ratio of 0.25 based on six points of intersection in Fig. 6.

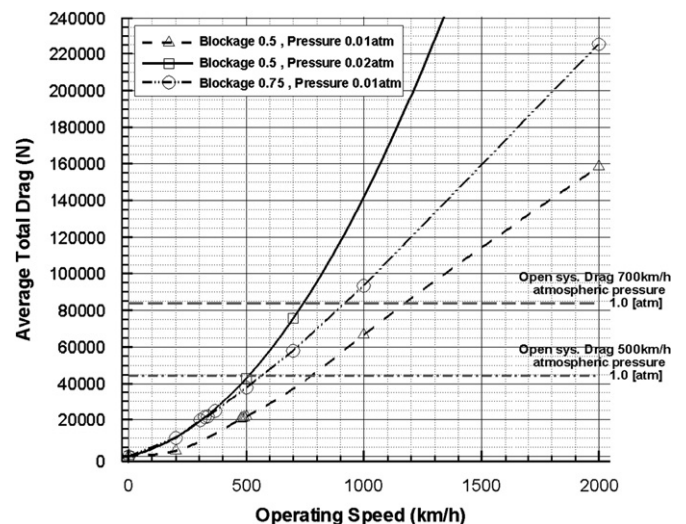


Fig. 8. The operating speed vs. the time averaged total drag with a blockage ratio of 0.5 and internal tube pressures of 0.01 and 0.02 atm and a blockage ratio of 0.75 and internal tube pressure of 0.01 atm.



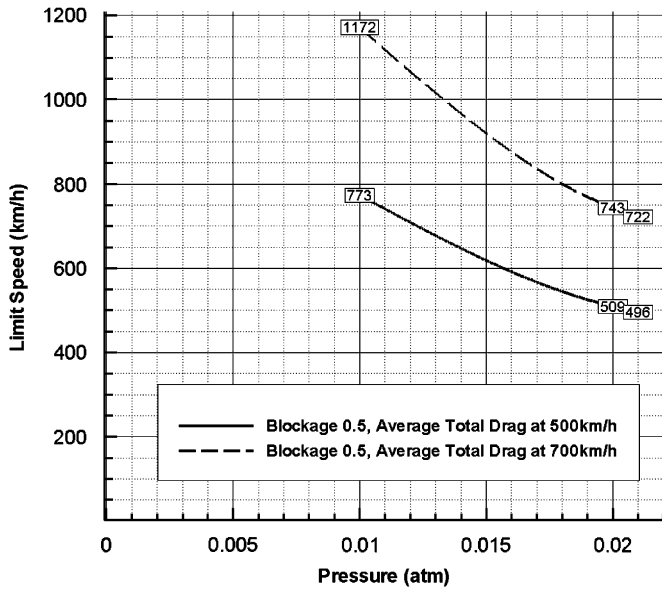


Fig. 9. The internal tube pressure vs. the limit speed with a blockage ratio of 0.5 based on six points of intersection in Fig. 8.

from which the aerodynamic drag and the operating speed of the tube train are decided.

The pressure drag is dominant in the case of low internal pressure of tube as mentioned in Section 3.1

$$D \propto V_{\infty}^2 \tag{6}$$

Hence, the average total drag tends to increase in proportion to the square of the operating speed in Figs. 6 and 8.

The case of a blockage ratio of 0.25 and pressure of 0.1 atm with an operating speed of 500 km/h is in the subsonic region where the Mach number of overall flow is between 0.61 and 0.66 and the total drag increases in proportion to  $V_{\infty}^2$ . However, the case of a blockage ratio of 0.25 and pressure of 0.1 atm with an operating speed of 1000 km/h is in the supersonic region where the Mach number of overall flow is between 1.45 and 1.62 in which case inflection occurs on the solid line when the normal shock becomes an oblique shock.

If internal tube pressure is changed, Eq. (6) can be expressed as

$$D \propto P_{\infty} V_{\infty}^2 \tag{7}$$

For the case of a constant drag, i.e., the drag of tube system is the same value with the drag of open system at intersection points in Fig. 6

$$V^2 \propto P \tag{8}$$

Therefore, the operating speed or limit speed tends to decrease as the internal tube pressure increases in Figs. 7 and 9.

### 3.3. The critical speed according to the blockage ratio and internal tube pressure

Aerodynamically, if a flow accelerates and then exceeds the speed of sound, shock waves possibly occur and the aerodynamic drag is dramatically increased. In existing ground transportation systems, shock-wave issues are not usually considered due to the relatively slow operating speed. However, in a tube train system, the shock-wave problem has to be taken into account because the tube train operates at very high speed in a restricted environment. In this study, the critical speed was defined as the speed at which shock waves occur in the tube train system. Shock waves occur between the vehicle and the tube wall when the speed of

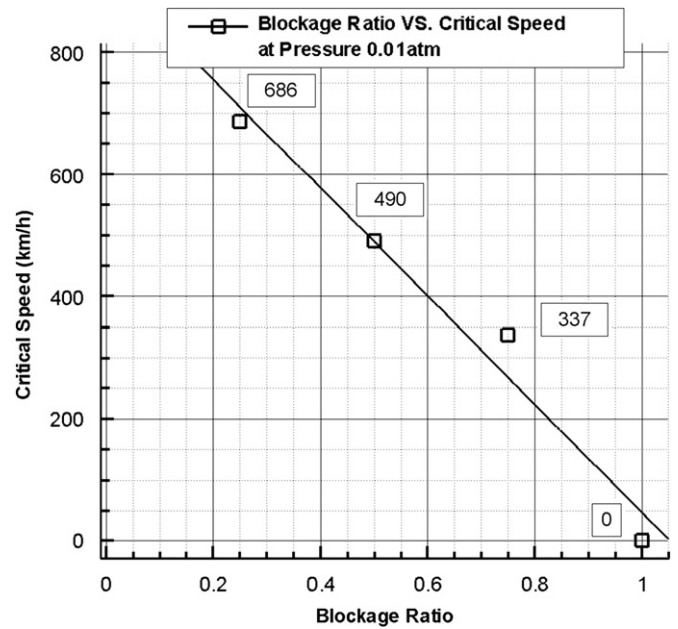


Fig. 10. The blockage ratio vs. the critical speed at an internal tube pressure of 0.01 atm.

the tube train exceeds the critical speed, as shown in Fig. 5; as a result, the average total drag is significantly increased due to the total pressure loss resulting from the shock waves. The critical speeds are shown in Fig. 10 for various blockage ratios when the internal tube pressure is 0.01 atm. When the operating speed is below the critical speed, the energy efficiency is competitive but the operating speed is relatively slow. On the other hand, when the operating speed is above the critical speed, the energy efficiency is not competitive but the operating speed can be improved relative to a ground vehicle. Therefore, the critical speed can be considered as one of the important parameters in the initial design state of a tube train for various purposes. They include personnel transportation for which the transit time is relatively important and cargo transportation for which energy efficiency is of particular interest.

The critical speed is mostly affected by the blockage ratio, which accelerates the flow inside the tube. However, the internal tube pressure has an inconsiderable effect on the critical speed, as shown in Eqs. (9)–(11). As shown in Fig. 10, the critical speed plunges as the blockage ratio rises. Through the results depicted in Fig. 10, the critical speed or operating speed of the tube train can be predicted by selecting the blockage ratio when the internal tube pressure is 0.01 atm. On the contrary, the blockage ratio can be estimated by selecting the critical speed or operating speed.

Generally,  $V_c$  can be written as Eq. (9)

$$V_c = f(M_c, Re, \beta) \tag{9}$$

where  $M_c = (V_c / \sqrt{\gamma RT})$ .

For a given initial temperature of internal tube, roughly

$$V_c = f(Re, \beta) \tag{10}$$

Since a shock structure including a critical speed is mainly affected by Mach number, but not Reynolds number, Eq. (10) becomes

$$V_c = f(\beta) \tag{11}$$

Hence, the critical speed is a function of only the blockage ratio and the effect of the pressure is almost nil.



#### 4. Discussion

In this study, investigations of a tube train system with huge size, long length, high operating speeds, and various internal tube pressures were performed by examining the aerodynamic characteristics of a tube train system and complementing the extant, inadequate literature prior to full-scale research into the tube train system in South Korea. As a result, the average total drag of each time, the required internal tube pressure, the critical speed that is directly related to the efficiency, and the limit speed of the tube train system were obtained by thoroughly examining a variety of cases of different blockage ratios, internal tube pressures, and operating speeds, which were the most important parameters of the initial design state.

In a tube train system unlike a ground system, the total drag is linearly proportional to the internal tube pressure and the square of the operating speed. Also, the total drag greatly increases and the efficiency sharply decreases when shock waves occur. However, in a tube train system, the total drag and the shock effect will be reduced and the operating speed will be improved, by keeping low the internal tube pressure. In addition, the operating speed is inversely proportional to the internal tube pressure and the blockage ratio. Moreover, the critical speed is in inverse proportion to the blockage ratio but the effect of the internal tube pressure is almost nil. For these reasons, the internal tube pressure should remain as low as possible and the blockage ratio also should be minimized in order to enhance the efficiency, which in this study was represented by the operating speed and the critical speed. For future work, the design optimization of the vehicle shape is also needed for the control of the shock waves.

Consequently, an ideal tube train system that has small driving resistance, fast operating speed, and high efficiency can be achieved when the internal tube pressure is very low as in a vacuum state and the blockage ratio is small. However, the internal tube pressure and the blockage ratio cannot be decreased infinitely. Hence, if the propulsion system is given and the operating speed is decided, we should consider the following two different design methods. The first design method is to enhance the aerodynamic characteristics by minimizing the aerodynamic drag due to shock waves. In this method, the operating speed is assumed as the critical speed, which is a criterion of efficiency, to suppress the generation of shock waves. Given the operating speed, the blockage ratio is calculated from the critical  $V$ - $\beta$  relation in Fig. 10. Then, the internal tube pressure is determined by the  $\beta$ - $P$  relation in Fig. 4. With the blockage ratio and the internal tube pressure being determined as above, the tube train system can finally be designed. However, as a result of the low operating speed, it is possible to realize a higher blockage ratio than the initial expectation. This increased blockage ratio leads to an increased cost of construction and maintenance of the low internal tube pressure. For future work, further studies on the optimization of the blockage ratio and the internal tube pressure are required for cost control. Another design method focuses on the economic aspects instead of the aerodynamic characteristics. For beneficial transportation, faster operating speeds of the tube train can be advantageous. Although a small blockage ratio is appropriate considering the aerodynamic aspects, the size of the train needs to be large enough for the purpose of personnel or cargo transportation. On the other hand, increasing the size of the tube (tunnel) increases the cost. For these reasons, it is hard to achieve the purpose of economical design by adjusting only the operating speed and the blockage ratio. Therefore, it can be an effective way of tube train design to lower the internal tube pressure, even if the blockage ratio rather increases and the operating speed sustains high. In this case, the amount of decompression can be introduced from the  $\beta$ - $P$

relation. To sum up, an integrated study that considers both aerodynamic and economic aspects is essential for the effective and competitive design of a tube train system.

#### 5. Conclusion

Aerodynamic characteristics were investigated with a tube train system of a huge size and long shape through computational analysis. The primary results were as follows:

- (1) The  $P$ - $D$  relation, viz., the relation between the internal tube pressure and the velocity-blockage ratio when the time averaged aerodynamic drag of the operating tube train had the same value as that of the open system.
- (2) The  $P$ - $\beta$  relation, viz., the relation between the internal tube pressure and the blockage ratio.
- (3) The  $D$ - $V$  relation, namely, the relation between the time averaged aerodynamic drag of the tube train and the operating speed for various cases of the blockage ratio-internal tube pressure.
- (4) The  $V$ - $P$  relation, i.e., the relation between the speeds (the limit speed and the operating speed) of the tube train and the internal tube pressure, which is required for the design of a tube train system.
- (5) The critical  $V$ - $\beta$  relation, which is the relation between the critical speed of the tube train and the blockage ratio when the Mach number of the local flow around the vehicle reaches unity.

In addition, the shock wave, which is one of the physical phenomena of internal tube flow, was also demonstrated. This study was of considerable importance because detailed aerodynamic characteristics of a tube train system with large length scales were presented for the first time even if the tube train shape was a simple geometry, i.e., a symmetric shape. Compared with existing study results, even if the vehicle shapes differ, the results of this study provided a number of data that included the critical speed, limit speed, average total drag,  $P$ - $D$  relation,  $P$ - $\beta$  relation,  $D$ - $V$  relation,  $V$ - $P$  relation, and critical  $V$ - $\beta$  relation, depending on various cases of the internal tube pressure, blockage ratio, and operating speed. Moreover, these results can be applied to other relative studies, actual system design and construction, and can also be used as guidelines, e.g., the critical speed, which was a bifurcation parameter between the purposes of personnel transportation and cargo transportation. Currently in South Korea, a tube train at an operating speed level of 700 km/h is required. Consequently, we confirmed that this tube train would operate with the same energy efficiency as that of current commercial magnetic levitation trains at the speed of 500 km/h if the tube train system is designed with an internal tube temperature of about 290 K, internal tube pressure under 0.025 atm, and blockage ratio under 0.25. Also, if the internal tube pressure is maintained at under 0.01 atm, a tube train that has an operating speed of 1000 km/h will be realized with a blockage ratio of 0.25 and the propulsion system of current commercial maglev trains. This paper proposes only technical considerations for conceptual design of tube train system with an operating speed, a blockage ratio and internal tube pressure. If costs of tube construction and operation of overall system including maintenance of pressure inside a tube are considered in the design stage, more realistic values of tube train system would be determined with economical evaluation.

#### Acknowledgements

This work was supported by the second stage of the Brain Korea 21 Project in 2011.

This work was supported by the New and Renewable Energy Program of the Korea Institute of Energy Technology Evaluation and Planning (KETEP) Grant funded by the Korea government Ministry of Knowledge Economy (No. 20104010100490).

This work was also supported by the National Research Foundation of Korea (NRF) Grant funded by the Korea Government (MEST) (No. 20110001227).

## References

- Arnone, Andrea, Liou, Meng-Sing, Povinelli, Louis A., 1995. Integration of Navier–Stokes equations using dual time stepping and a multigrid method. *AIAA Journal* 33 (6), 985–990.
- Bourquin, Vincent, Alexis Monkewitz, Peter, 1999. Reduced-Scale Aerodynamic Testing of High-Speed Vehicles in Tunnels. Ph.D. Dissertation. Ecole Polytechnique fédérale de Lausanne EPFL. No. 1973.
- Harman, Charles M., Davidson, James V., 1977. The drag on vehicle in tunnels. *High Speed Ground Transportation Journal* 11 (2), 177–187.
- Kim, T.K., 2008. Aerodynamic Characteristics of a Tube Transportation System. MA Dissertation. Department of Mechanical and Aerospace Engineering, Seoul National University.
- Kwon, Hyeok-Bin, Park, Jun-Seo, Nam, Seong-Won, Choe, Seong-Gyu, 2008. (The) Current status and future prospect of the tube transportation technology. *Journal of the Korean Society for Railway* 1229-110211 (3), 59–71.
- Kwon, Hyeok-Bin, 2008. (A) Study on the Tube Transportation Technology, Korea Railroad Research Institute.
- Kwak, Rogers, 1990. Upwind differencing scheme for the time-accurate incompressible Navier–Stokes equations. *AIAA Journal* 28 (2), 253–262.
- Lee, Jinsun, Lim, Kwansu, Nam, Doohee, Kwon, Hyukbin, kim, Jungyeol, 2008. Economic feasibility and basic technical requirements for tube transportation system. *Journal of the Korean Society for Railway* 11 (5), 513–518.
- Lee, Bo-Sung, Lee, Dong-Ho, 1998. Parallel Computations on Steady/Unsteady Turbulent Flows around Two-Dimensional Transonic Airfoils, KAIA.
- Lever, James H., 1998. Technical Assessment of Maglev System Concepts. Final Report by the Government Maglev System Assessment Team, US Army Corps of Engineers (Special Report 98-12). Retrieved 23.05.07. <<http://www.swissmetro.ch>>.
- Retrieved 23.04.07. <[http://www.cargocap.de/index\\_en.html](http://www.cargocap.de/index_en.html)>.
- Retrieved 03.05.09. <[www.buispost.eu](http://www.buispost.eu)>.
- Retrieved 03.05.09. <[www.pevco.com](http://www.pevco.com)>.
- Retrieved 29.05.07. <[http://www.cbruch.homepage.t-online.de/Rumba\\_e.html](http://www.cbruch.homepage.t-online.de/Rumba_e.html)>.
- Retrieved 06.12.07. <<http://www.et3.com>>.
- Retrieved 05.12.07. <[http://www.pe.com/multimedia/flash/2006/20060430\\_transportation/TRANSFINAL.swf](http://www.pe.com/multimedia/flash/2006/20060430_transportation/TRANSFINAL.swf)>.
- Retrieved 24.04.07. <<http://www.pipenet.it>>.
- Rumsey, Christopher L., Sanetrik, Mark D., Biedron, Robert T., Melson, N. Duane, Parlette, Edward B., 1995. Efficient and Accuracy of Time-Accurate Turbulent Navier–Stokes Computations. *AIAA* 95-1835 (June). Retrieved 20.08.08. <<http://www.transrapid.de>>.
- Sung Kim, Chang, 2001. Sensitivity Analysis for the Navier–Stokes Equations with Two-Equation Turbulence Models and Its Applications. Ph.D. Dissertation. Department of Mechanical and Aerospace Engineering, Seoul National University.
- Trzaskoma, W.P., 1970. Tube Vehicle System (TVS) Technology Review. MITRE Report No. M70-4, July, NTIS No. PB 193–451.